Journal of Computational Electronics 1: 81–85, 2002
© 2002 Kluwer Academic Publishers. *Manufactured in The Netherlands.*

Towards Fully Quantum Mechanical 3D Device Simulations

M. SABATHIL, S. HACKENBUCHNER, J.A. MAJEWSKI, G. ZANDLER AND P. VOGL
Walter Schottky Institute and Physics Department, Technical University of Munich, Am Coulombwall, 85748 Garching, Germany

Abstract. We present a simulator for calculating, in a consistent manner, the realistic electronic structure of three-dimensional heterostructure quantum devices under bias and its current density close to equilibrium. The electronic structure is calculated fully quantum mechanically, whereas the current is determined by employing a semiclassical concept of local Fermi levels that are calculated self-consistently. We discuss the numerical techniques employed and present illustrative examples that are compared with quantum transport calculations. In addition, the simulator has been used successfully to study shape-dependent charge localization effects in self-assembled GaAs/InGaAs quantum dots.

Keywords: nano-devices, simulations, quantum dots

1. Introduction

State-of-the-art simulators for semiconductor nano-structures and optoelectronic nano-devices roughly fall into two classes (Anonymous 2000): some models focus on the *equilibrium* electronic structure. They attempt to predict, as accurately as possible, the free and bound charge density as well as optical properties of quantum wells, wires, and dots on a length scale that ranges from nm to μm. Several models of this kind have been developed in the last few years that can deal with fully three-dimensional device geometries, and invoke one-band (Kumar, Laux and Stern 1990, Laux 1987), or several-band $k \cdot p$ models (Grundmann, Stier and Bimberg 1999, Pryor 1998, 1999, Cusack, Briddon and Jaros 1996), tight binding methods (Carlo 2001). The second class of models focus on *current-voltage characteristics* and attempts to solve quantum transport equations, using non-equilibrium Green functions (Lake *et al.* 1997, Klimeck, Lake and Blanks 1998), Wigner functions (Bordone *et al.* 1999, Grubin, Buggeln and Kreskovsky 2000, Ferry, Akis and Vasileska 2000), or the Pauli master equation (Fischetti 1998, 1999). Presently, they are still limited to one spatial dimension and/or put less emphasis on details of the electronic structure. Thus, a simultaneous realistic treatment of the electronic structure and the quantum transport problem for 3-D structures still poses a challenging task.

In this paper we discuss a simulator that we are currently developing for a wide class of 3-D Si and III-V nano-structures (Hackenbuchner *et al.* 2001). It attempts to bridge the two types of approaches described above, albeit with a stringent limitation that makes it feasible to simulate three-dimensional structures: we solve the electronic structure problem accurately but restrict the current evaluation to situations close to equilibrium where the concept of local quasi-Fermi levels is still justifiable. This approach may be viewed as a low-field approximation to the Pauli master equation (Jones and March 1973). In this paper, we present the numerical methods involved, illustrate this method for simple 1-D situations that allow a detailed comparison with the full Pauli master equation approach that has recently been developed by Fischetti (1998, 1999), and briefly show that this simulator successfully predicts the electronic and optical properties of self-assembled GaAs/InAs quantum dots.

2. Method

The nano-device simulator that we have developed so far solves the 8-band-$k \cdot p$-Schrödinger-Poisson equation for arbitrarily shaped 3-D heterostructure device

geometries, and for any (III-V and Si/Ge) combination of materials and alloys. It includes band offsets of the minimal and higher band edges, absolute deformation potentials (Van de Walle 1989), local density exchange and correlations (i.e. the Kohn-Sham equations), total elastic strain energy (Pryor *et al.* 1998, Grundmann, Stier and Bimberg 1995) that is minimized for the whole device, the long-range Hartree potential induced by charged impurity distributions, voltage induced charge redistributions, piezo- and pyroelectric charges, as well as surface charges, in a fully self-consistent manner. The charge density is calculated for a given applied voltage by assuming the carriers to be in a *local* equilibrium that is characterized by energy-band dependent local quasi-Fermi levels $E_{\mathrm{Fc}}(\mathbf{x})$ for charge carriers of type c (i.e. in the simplest case, one for holes and one for electrons),

$$n_c(\mathbf{x}) = \sum_i |\Psi_{ic}(\mathbf{x})|^2 f\left(\frac{E_{\mathrm{Fc}}(\mathbf{x}) - E_{ic}}{k_B T}\right). \qquad (1)$$

These local quasi-Fermi levels are determined by global current conservation $\nabla \cdot \mathbf{j}_c = 0$, where the current is assumed to be given by the semi-classical relation $\mathbf{j}_c(\mathbf{x}) = \mu_c n_c(\mathbf{x}) \nabla E_{\mathrm{Fc}}(\mathbf{x})$ (see, e.g. (Selberherr 1984)). Recombination and generation processes are included additionally. The carrier wave functions Ψ_{ic} and energies E_{ic} are calculated by solving the multi-band Schrödinger-Poisson equation. The open system is mimicked by using mixed Dirichlet and von Neumann boundary conditions (Fischetti 1998, Lent and Kirkner 1990, Frensley 1992) at Ohmic contacts.

3. Computational Schemes

For a given nano-structure, the computations start by globally minimizing the total elastic energy (Pryor *et al.* 1998, Grundmann, Stier and Bimberg 1995) using a conjugate gradient method. This determines the piezo-induced charge distributions, the deformation potentials and band offsets. Subsequently, the 8-band-Schrödinger, Poisson, and current continuity equations are solved iteratively. All equations are discretized according to the finite difference method invoking the box integration scheme (Kumar, Laux and Stern 1990, Laux 1987, Selberherr 1984). The irregular rectilinear mesh is kept fixed during the calculations. As a preparatory step, the built-in potential is calculated for zero applied bias by solving the Schrödinger and Poisson equation self-consistently employing a predictor-corrector approach (Trellakis *et al.* 1997) and setting to zero the electric field at the Ohmic contacts. For applied bias, the Fermi level and the potential at the contacts are then shifted according to the applied potential which fixes the boundary conditions. The main iteration scheme itself consists of two parts. In the first part, the wave functions and potential are kept fixed and the quasi-Fermi levels are calculated self-consistently from the current continuity equations, employing a conjugate gradient method and a simple relaxation scheme. In the second part, the quasi-Fermi levels are kept constant, and the density and the potential are calculated self-consistently from the Schrödinger and Poisson equation. The discrete 8-band-Schrödinger equation represents a huge sparse matrix (typically of dimension 10^5 for 3D-structures) and is diagonalized using the Jacobi-Davidson method (Bai *et al.* 2000) that yields the required inner eigenvalues and eigenfunctions close to the energy gap. We very slightly shift the spin-up and spin-down diagonal Hamiltonian matrix elements with respect to each other in order to avoid degeneracies and guarantee orthogonal eigenstates automatically. To reduce the number of necessary diagonalizations, we employ an efficient predictor-corrector approach (Trellakis *et al.* 1997) to calculate the potential from the nonlinear Poisson equation. In this approach, the wave functions are kept fixed within one iteration and the density is calculated perturbatively from the wave functions of the previous iteration (Trellakis *et al.* 1997). The nonlinear Poisson equation is solved using a modified Newton method, employing a conjugate gradient method and line minimizations. The code is written in Fortran 90 and consists of some 170000 lines by now.

4. One-Dimensional Examples and Comparison to Pauli Master Approach

In this section we illustrate the present method by studying simple one-dimensional examples that we can compare to full Pauli master equation results (Fischetti 1998). As discussed above, our method amounts to calculating the electronic structure of a device fully quantum mechanically, yet employing a semiclassical scheme for the evaluation of the current. As we shall see, the results are close to those obtained by the full Pauli master equation (Fischetti 1998) provided we limit ourselves to situations not too far from equilibrium.

As a first example, we consider a one-dimensional (Si-based) n-i-n structure (Fig. 1) at room temperature

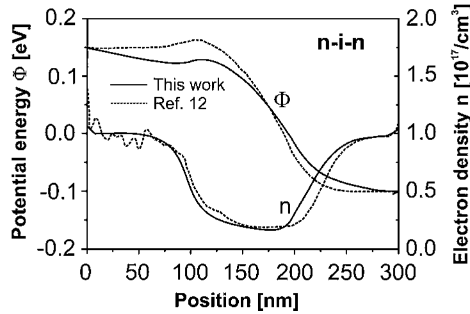

Figure 1. Calculated potential energy and electron density of n-i-n structure, as a function of position inside the structure. Results from presently developed method (full lines) are compared to results from Pauli master equation (Fischetti 1998) (dashed lines).

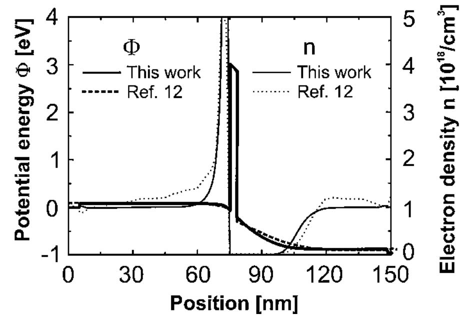

Figure 2. Calculated potential energy Φ and electron density n of Si-SiO_2-Si structure with 3 nm barrier, as a function of position inside the structure. Results from presently developed method (full lines) are compared to results from Pauli-master equation (Fischetti 1998) (dashed lines).

with 100 nm long n-typed regions and a doping concentration of $n = 10^{17}$ cm^{-3}. The applied bias is 0.25 V. As one may expect, true quantum mechanical effects play little role in this case and both the present, the semiclassical drift-diffusion as well as the Pauli master equation (PME) approach of Fischetti (1998) yield practically identical results for the density and potential profile. We would like to point out, that this good agreement is a nontrivial finding, as we calculate the density quantum mechanically according to Eq. (1) with self-consistently computed local Fermi levels rather than semiclassically. Our current density of 3.6×10^4 A/cm^2 compares well with the PME result of 6.8×10^4 A/cm^2. However, we note that the current is directly proportional to the mobility in our model; changing the mobility (that we treat as constant in this example) therefore changes the value of the current but does not affect the electron density or potential profile.

In Fig. 2 we show results for a Si-SiO_2-Si structure with a 3 nm barrier of 3 eV height and a forward bias of 1 V. Again, our calculated density and potential profile can be seen to agree very well with the PME method (Fischetti 1998). Due to the high barrier, the current density predicted by the PME is only of the order of 10^{-8} A/cm^2. In our approach, the tunneling current density is still small but significantly higher (10^{-3} A/cm^2). This originates in our simplified treatment of boundary conditions which mimic an open system by linearly combining stationary (non-current carrying) solutions of the Schrödinger equation with von Neumann and Dirichlet boundary conditions at the contacts (Lent and Kirkner 1990, Frensley 1992). For a high barrier near the middle of the device, the minimum electron density for zero or small bias lies near the center of the barrier irrespective of the boundary conditions used. This is in contrast to current carrying scattering solutions that travel from left to right (right to left) and reach their minimum at the right (left) side of the barrier. While this difference has practically no effect on the potential and density outside the barrier, it raises the tunneling current significantly for small bias and very high barriers. We are currently generalizing our approach by filtering out scattering states from the stationary Schrödinger solutions and deriving appropriate open boundary conditions, in analogy to very recent work of Laux and Fischetti (unpublished).

Finally, we study the same n-i-n structure as in Fig. 1, but with an additional well of 10 nm width and 0.1 eV depth. Figure 3 shows the potential profile. The well supports three strongly localized states. Quantum mechanics yields a smaller electron density

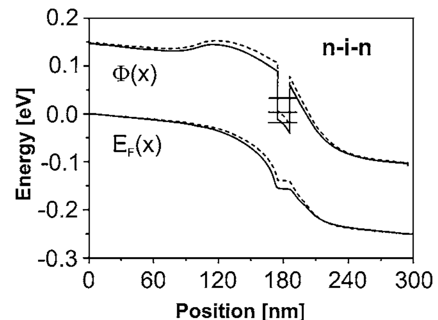

Figure 3. Calculated potential energy Φ and local electron Fermi level E_F with a 10 nm wide quantum well for a n-i-n structure as a function of position. The full line is obtained with the present method, whereas the dashed line shows the classical drift-diffusion solution. Also shown are the positions of the three localized energy levels of the well.

in the well region than the classical Thomas-Fermi (drift-diffusion) solution which is a physically plausible result. This leads to a larger potential drop across the well region which in turn results in a higher current density J. The classical drift-diffusion solution gives $J = 2.2 \times 10^4$ A/cm^2 whereas the present model gives $J = 2.5 \times 10^4$ A/cm^2. The localized states themselves contribute very little to the current. As a consequence, the local Fermi level is practically constant across the bound states which provides an a-posteriory justification of invoking non-local quantum mechanics concurrently with the semi-classical concept of local Fermi levels. In fact, no conflict arises for situations close to equilibrium since the spatial variation of the occupancy of any given eigenstate turns out to be negligible for three reasons: (i) Deeply bound states do not contribute to the current and thus do not lead to a gradient of the Fermi level; (ii) the Fermi level has the largest variation in regions where the density is very low (within barriers, for example); (iii) very extended states that are treated formally as bound states in our method are either not occupied because of their high energy, or occur in regions of high density (near contacts, for example) where the quasi-Fermi level is nearly constant.

In summary, the electronic density and potential calculated with the presently developed scheme as a function of applied bias agrees excellently with the more rigorous Pauli master equation approach. More work will be needed, on the other hand, to model ultrasmall tunneling currents accurately.

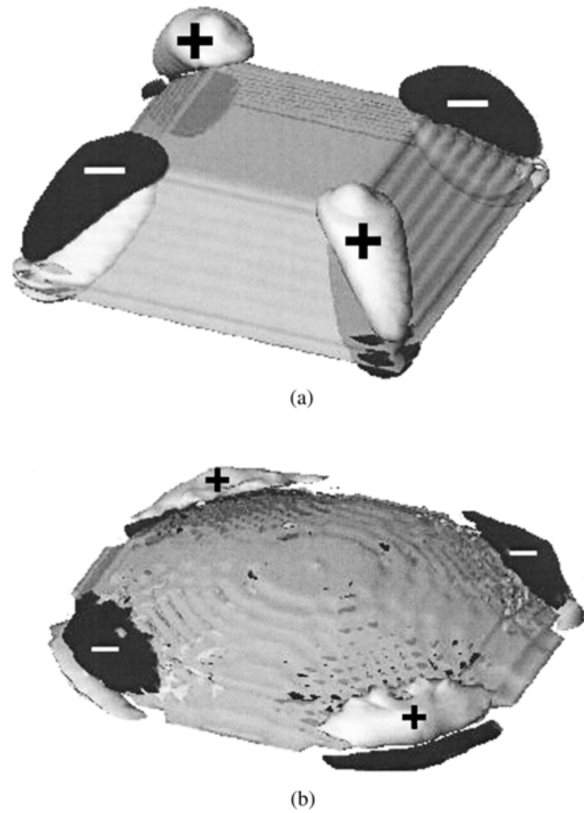

Figure 4. Side view of calculated (a) pyramid-shaped and (b) lens-shaped InGaAs quantum dots. The height in the center is 8 nm for both dot shapes. The light and dark regions are iso-surfaces of the positive and negative piezoelectric charge densities, respectively, with a magnitude of 5×10^{18} e/cm^3.

5. Piezoelectric Fields and Electron-Hole Localization in Quantum Dots

We have applied our simulator to study theoretically single-quantum-dot photodiodes consisting of self-assembled InGaAs quantum dots with a diameter of 30–40 nm and heights of 4–8 nm that are embedded in the intrinsic region of a Schottky diode (Hackenbuchner *et al.* 2001). Recent experiments (Findeis *et al.* 2001, Fry *et al.* 2000) have indicated inverted electron-hole alignments with the electron at the base and the hole at the top of the dot, in contrast to what earlier theoretical calculations (Pryor 1998, 1999, Cusack, Briddon and Jaros 1996, Jones and March 1973) had predicted. Our study reveals that the elastic strain and accompanying piezoelectric fields strongly depend on the geometric shape and alloy composition of dots. We find, in agreement with (Grundmann, Stier and Bimberg 1999), dots of pyramidal shape to possess large piezoelectric polarization charges in the corners that lead to a strong hole confinement near the dot edges (Fig. 4(a)). By contrast, lens-shaped dots of similar size have much weaker charges and are found to lead to electron *and* hole states near the center of the lens which significantly improves the exciton absorption (Fig. 1(b)). Importantly, as we have shown elsewhere (Hackenbuchner *et al.* 2001), we find the hole to be localized at the apex (top) and the electron at the base exactly as has been suggested by Fry *et al.* (2000).

Acknowledgments

Financial support by the Deutsche Forschungsgemeinschaft and by the Office of Naval Research under Contract No. N00014-01-1-0242 is gratefully

acknowledged. We are indebted to Frank Stern for helpful discussions in the early stage of the project.

References

Anonymous. 2000. In: Proc. of the 7th Int. Workshop on Computational Electronics, Glasgow, Scotland, May 22–25, 2000 and papers therein.

Bai Z., Demmel J., Dongarra J., Ruhe A., and van der Vorst H. (Eds.). 2000. Templates for the Solution of Algebraic Eigenvalue Problems. SIAM, Philadelphia.

Bordone P., Pascoli M., Brunetti R., Bertoni A., Jacoboni C., and Abramo A. 1999. Phys. Rev. B 59: 3060.

Cusack M.A., Briddon P.R., and Jaros M. 1996. Phys. Rev. B 54: R2300.

Di Carlo A. 2001. Proc. 12th Int. Conf. on Nonequilibrium Carrier Dynamics in Semiconductors, Santa Fe, 2001, also to appear in Physica B.

Ferry D.K., Akis R., and Vasileska D. 2000. Electron Device Meeting, IEDM 2000 Tech. Digest Papers, pp. 287–290.

Findeis F., Baier M., Beham E., Zrenner A., and Abstreiter G. 2001. Appl. Phys. Lett. 78: 2958.

Fischetti M.V. 1998. J. Appl. Phys. 83: 270.

Fischetti M.V. 1999. Phys. Rev. B 59: 4901.

Frensley W.R. 1992. Superlattices and Microstructures 11: 3470.

Fry P.W., Itskevich I.E., Mowbray D.J. *et al*. 2000. Phys. Rev. Lett. 84: 733.

Grubin H.L., Buggeln R.C., and Kreskovsky J.P. 2000. Superlattices and Microstructures 27: 533.

Grundmann M., Stier O., and Bimberg D. 1995. Phys. Rev. B 52: 11969.

Grundmann M., Stier O., and Bimberg D. 1999. Phys. Rev. B 59: 5688.

Hackenbuchner S., Sabathil M., Majewski J.A., Zandler G., Vogl P., Beham E., Zrenner A., and Lugli P. 2001. Proc. 12th Int. Conf. on Nonequilibrium Carrier Dynamics in Semiconductors, Santa Fe, 2001, also appear Physica B.

Jones W. and March N.H. 1973. Theoretical Solid State Physics. Wiley, Vol. 2.

Klimeck G., Lake R., and Blanks D.K. 1998. Phys. Rev. B 58: 7279.

Kumar A., Laux S.E., and Stern F. 1990. Phys. Rev. B 42: 5166; Laux S.E. 1987. In: Miller J.J.H. (Ed.), Proc. 5th Int. Conf. on Numerical Analysis of Semiconductor Devices and Integrated Circuits (NASECODE V), Boole, Dun Laoghaire, Ireland, pp. 270–275.

Lake R., Klimeck G., Bowen R.C., and Jovanovic D. 1997. J. Appl. Phys. 81: 7845; Project “NEMO”, http://www.cfdrc.com/nemo/index.html.

Laux S. and Fischetti M.V. Presented at this conference, unpublished.

Lent C.S. and Kirkner D.J. 1990. J. Appl. Phys. 67: 6353.

Pryor C. 1999. Phys. Rev. B 57: 7190.

Pryor C. 1999. Phys. Rev. B 60: 2869.

Pryor C., Kim J., Wang L.W., Williamson A.J., and Zunger A. 1998. J. Appl. Phys. 83: 2548.

Selberherr S. 1984. Analysis and Simulation of Semiconductor Devices. Wien, Springer.

Trellakis A., Galick A.T., Pacelli A., and Ravaioli U. 1997. J. Appl. Phys. 81: 7880.

Van de Walle C. 1989. Phys. Rev. B 39: 1871.